NANO LETTERS

Letter

pubs.acs.org/NanoLett

Room-Temperature Voltage Tunable Phonon Thermal Conductivity via Reconfigurable Interfaces in Ferroelectric Thin Films

Jon F. Ihlefeld,*[,†] Brian M. Foley,[‡] David A. Scrymgeour,[†] Joseph R. Michael,[†] Bonnie B. McKenzie,[†] Douglas L. Medlin,[§] Margeaux Wallace,[∥] Susan Trolier-McKinstry,[∥] and Patrick E. Hopkins*[,‡]

[†]Sandia National Laboratories, Albuquerque, New Mexico 87185 United States

[‡]Department of Mechanical and Aerospace Engineering, University of Virginia, Charlottesville, Virginia 22904 United States

[§]Sandia National Laboratories, Livermore, California 94550 United States

[∥]Department of Materials Science and Engineering, The Pennsylvania State University, University Park, Pennsylvania 16802 United States

S *Supporting Information*

ABSTRACT: Dynamic control of thermal transport in solid-state systems is a transformative capability with the promise to propel technologies including phononic logic, thermal management, and energy harvesting. A solid-state solution to rapidly manipulate phonons has escaped the scientific community. We demonstrate active and reversible tuning of thermal conductivity by manipulating the nanoscale ferroelastic domain structure of a $Pb(Zr_{0.3}Ti_{0.7})O_3$ film with applied electric fields. With subsecond response times, the room-temperature thermal conductivity was modulated by 11%.

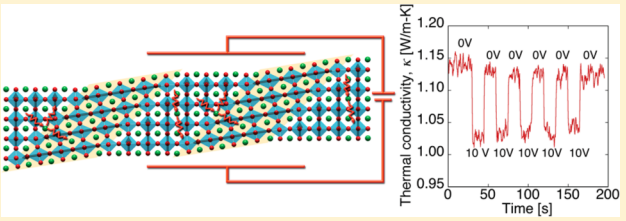

KEYWORDS: *Thermal conductivity, tunable, time domain thermoreflectance, ferroelectric, nano domain*

Dynamically regulating phonon transport in solids enables possibilities of thermal energy control, new computing mechanisms utilizing phonons, and a novel means to control phonon-coupled waves and particles such as polaritons and polarons.[1,2] Tuning phonon transport over a broad temperature range in a single solid-state device provides the largest technological and scientific impact. Prior to the present study, however, a solid-state solution to rapidly manipulate phonons has remained elusive. For example, solid-state thermal rectification at room temperature has been demonstrated,[3] but switching, gating, or dynamic tuning elements have escaped the scientific community. While it is possible to alter thermal conductivity through phase transitions,[4,5] chemical composition modification,[6] and cryogenically applied magnetic or electric fields,[7−11] none of these prior demonstrations provide a response that is sufficiently swift and facile for implementation across a wide-ranging application landscape. For example, in conventional ferroelectrics, mobile coherent interfaces, the ferroelastic domain walls, will scatter heat-carrying phonons, an effect that has previously been attributed to an acoustic mismatch across the interface,[10,12] but also likely has a significant strain[13] and accompanying decreased phonon relaxation time contribution.[14] Reconfiguring the domain walls with an electric field will alter the thermal conductivity, as was demonstrated in bulk, single crystalline barium titanate where thermal conductivity values increased by a factor of 5 after application of an electric field.[10] However, this effect was only present up to the temperature where Umklapp scattering became the dominant phonon scattering mechanism (∼30 K) and heretofore was limited to cryogenic temperature regimes.

If properly engineered, mobile phonon scattering interfaces would allow for tuning across much broader temperature ranges. To actively and practically achieve this goal requires the domain wall spacing to be comparable to or less than the phonon mean free path. Phonon mean free paths are known to be spectral and therefore have many wavelengths carrying thermal energy[15−18] but for a complex oxide it can be anticipated that most of these heat-carrying modes have lengths less than 100 nm at room temperature.[19−22] Decreasing domain wall spacing to this dimension requires scaling of the ferroelectric crystal size to increase domain wall density and decrease interface spacing to less than this dimension, which can be achieved in a thin film embodiment. Recently, we demonstrated that 30 nm thick epitaxial films of ferroelectric $BiFeO_3$ with differing densities of 71° domain walls showed ∼30% differences in thermal conductivity at temperatures up to 400 K, indicating domain wall phonon scattering effects may be observed at noncryogenic temperatures.[23] Reconfiguring the nanoscale domain structure and domain wall density with an applied field would allow the creation of a simple and integrable thermal switch that could operate over a broad temperature range. This requires a material system and embodiment where the domain structure can be reconfigured. In this Letter, we

Received: November 24, 2014
Revised: January 19, 2015
Published: February 19, 2015

DOI: 10.1021/nl504505t
Nano Lett. 2015, 15, 1791−1795

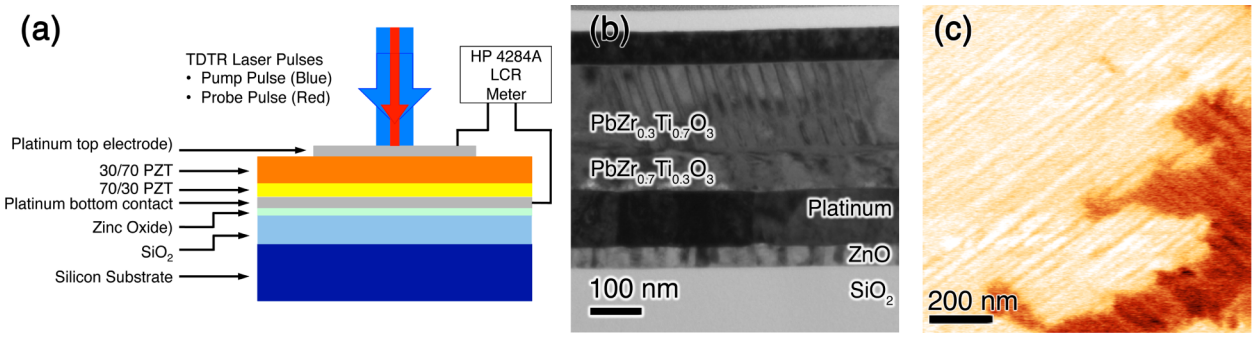

Figure 1. (a) Experimental geometry showing cross section of PZT bilayer sample. (b) Bright-field transmission electron micrograph of a PZT bilayer film imaged in cross-section showing a stripe pattern of 90° ferroelastic domains in the upper $PbZr_{0.3}Ti_{0.7}O_3$ layer. (c) Vertical piezoresponse force microscopy image showing the ferroelectric stripe domain structure of a PZT bilayer film.

present such an embodiment and demonstrate the tuning of phonon transport at room temperature by altering domain wall density with an electric field in a ferroelectric thin film.

Figure 1a shows the experiment geometry. Polycrystalline lead zirconate titanate (PZT) bilayer thin films composed of a tetragonal symmetry PZT layer ($PbZr_{0.3}Ti_{0.7}O_3$) on top of a rhombohedral symmetry PZT layer ($PbZr_{0.7}Ti_{0.3}O_3$) were used in this study as these have previously been shown to possess highly mobile ferroelastic domain walls with sub-100 nm spacing.[24] Films were deposited onto platinized silicon wafers (100 nm Pt/40 nm ZnO/400 nm SiO_2/Si (001)) with $PbZr_{0.3}Ti_{0.7}O_3$ thicknesses of 142 ± 3 nm and $PbZr_{0.7}Ti_{0.3}O_3$ thicknesses of 57 ± 4 nm, as determined using transmission electron microscopy (TEM). The films were randomly oriented as assessed by X-ray diffraction and clearly showed field-dependent polarization hysteresis, as shown in the Supporting Information. Platinum electrodes were prepared on the film surface to develop metal−insulator−metal structures for electrical and thermal characterization. Thermal conductivity was measured using time domain thermoreflectance (TDTR) using the platinum electrodes as transducer pads with which to measure and dynamically monitor the film thermal conductivity.[25−27] Direct current (dc) electric fields of up to 475 kV/cm were applied between the top and bottom platinum electrodes during these measurements. The TDTR data collected under the applied electric fields were then fit to a multilayer thermal model to determine the thermal conductivity of the $PbZr_{0.3}Ti_{0.7}O_3$ top layer. We are able to isolate our sensitivity to the thermal conductivity of this layer based on measurements made on separate calibration samples to determine the thermal conductivity of the $PbZr_{0.7}Ti_{0.3}O_3$ bottom layer and the conductance between this layer and the bottom platinum electrode. Additionally, the choice of modulation frequency (2.57 MHz) was made to minimize the sensitivity of the measurement to the interface conductance between the top platinum electrode and the $PbZr_{0.3}Ti_{0.7}O_3$ top layer relative to the sensitivity to the thermal conductivity of the $PbZr_{0.3}Ti_{0.7}O_3$ top layer. In our analysis, we assume that the thermal boundary conductance between the $PbZr_{0.3}Ti_{0.7}O_3$ and $PbZr_{0.7}Ti_{0.3}O_3$ layers is essentially infinite ($>1 \times 10^9$ W m^{-2} K^{-1}). While we expect that this is not the case in actuality, this assumption is made because we are unable to definitively characterize domain structure across the interface between the PZT layers via the techniques available. As a result, any possible effects localized near the interface specifically are lumped into the overall conductivity of the $PbZr_{0.3}Ti_{0.7}O_3$ top layer.

Figure 1b shows a bright-field TEM image where parallel bands of contrast consistent with ferroelastic domain structure are observed within the upper $PbZr_{0.3}Ti_{0.7}O_3$ layer. Crystallographic orientation analysis of the stripe contrast, as deduced from selected area electron diffraction (see Supporting Information), shows that these stripes are interfaces and are consistent with 90° ferroelastic domain walls, which lie parallel with {101} type planes in the tetragonal $PbZr_{0.3}Ti_{0.7}O_3$ phase.[28] The presence of distinct domains in the $PbZr_{0.3}Ti_{0.7}O_3$ layer is consistent with prior work on similar films.[24,29] The spacing of the domain walls as measured across multiple TEM micrographs ranges from ∼5 to 36 nm with a mean spacing of 16.5 ± 6.6 nm. A piezoresponse force microscopy (PFM) image of the film surface is shown in Figure 1c, where distinct stripe domains can be observed. The intensity of the out-of-plane PFM response was measured perpendicular to the stripe direction and reveals a mean domain wall spacing of 30.4 ± 3.3 nm for this particular region. The domain wall spacings varied depending upon the region measured but were consistent with those observed in the TEM images. Note that the measured spacings are subject to errors since, in general, the domain walls were not imaged edge-on in TEM or PFM; the measurement does, however, provide a confirmation of the nanoscale spacing.

Figure 2a shows the field dependence of thermal conductivity for the tetragonal $PbZr_{0.3}Ti_{0.7}O_3$ layer of the bilayer film. The error bars represent the uncertainty in the measurement over five TDTR scans performed at each applied field. For each device, the laser spot was focused onto the top surface of the platinum top electrode and was left in the same spot for all of the applied field conditions. This was done to reduce uncertainty due to variations in the thickness of the platinum top electrode that would need to be included had the measurement location changed on every scan; this resulted in much tighter error bars than a typical TDTR experiment as we alleviate the main source of experimental variation and uncertainty by fixing the measurement location on the sample when applying the electric field. The thermal conductivity decreases by 11% from the unpoled, virgin state under an applied field of 475 kV/cm. Upon removal of the applied field, it is found that the thermal conductivity does not recover fully to its original value, but that the thermal conductivity in the remanent poled, ferroelectric state is ∼2.7% less than that in the unpoled state. To study the speed and reproducibility of the field-induced thermal conductivity change, we monitored the thermoreflectivity of the top electrode at a fixed pump−probe delay time of 150 ps while cycling the applied dc field between

DOI: 10.1021/nl504505t
Nano Lett. 2015, 15, 1791−1795

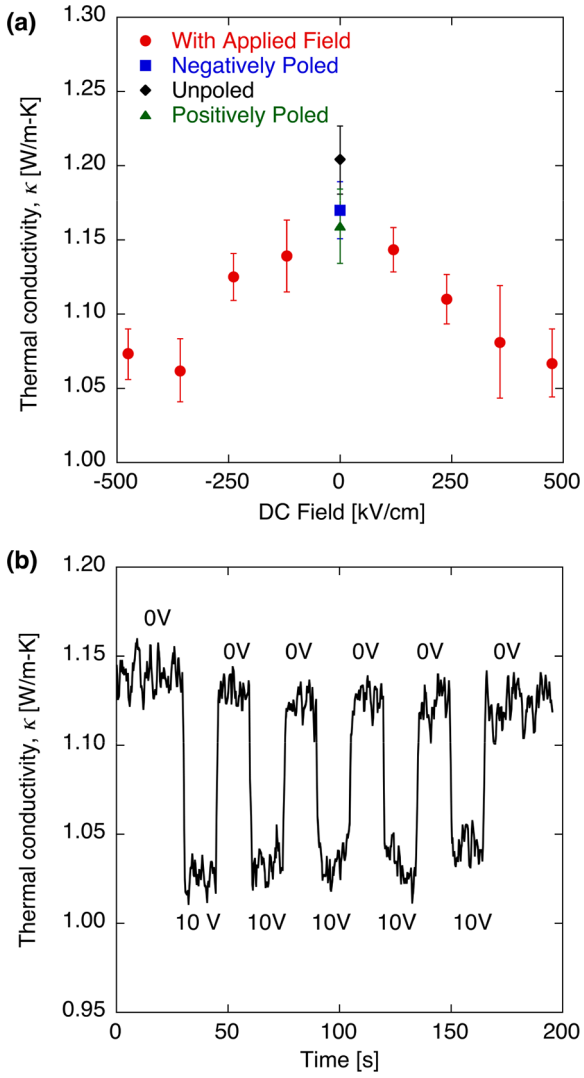

Figure 2. (a) dc electric field dependence of thermal conductivity in the $PbZr_{0.3}Ti_{0.7}O_3$ layer of the PZT bilayer film measured at room temperature (red circles). Also shown are the zero-field thermal conductivities of the initially unpoled material (black diamond) and those of the remanent, poled, material after application of positive (green triangle) and negative bias (blue square). (b) Real-time change in thermal conductivity measured via TDTR at a pump−probe delay time of 150 ps, showing the dynamic response of the thermal conductivity tuning effect.

0 and 475 kV/cm (0 and 10 V) and plotted the thermal conductivity as a function of time in Figure 2b. We observe a nearly instantaneous decrease (less than 300 ms, limited by the integration time of the lock-in amplifier) in the thermal conductivity when the field is applied, which recovers when the field is removed. This demonstrates that the thermal conduction decrease is rapid and recoverable between the poled (remanent) and applied-field states.

To demonstrate the mechanism for this result, we characterized the domain structure before and after poling with PFM and in operando during application of electric fields with channeling contrast scanning electron microscopy (SEM). The PFM measurements were performed with a conductive tip and no top electrode. The channeling contrast measurements utilized a 3 nm thick platinum electrode, which is thin enough to enable sufficient transparency for electron imaging, but thick enough to apply a field across the PZT film. Figure 3a,b shows a PFM image of a representative region of a bilayer film prior-to and after poling. Edge identification was used to measure the domain wall length before and after application of the field. Depending on the region measured, we observe −4.1 to +8.3% changes in domain wall line length/unit area after poling of the sample with an overall average increase of 2.6%. Figure 3c−f shows channeling contrast SEM images in states of negatively poled (negative remanent ferroelectric state), positive applied field, positively poled (positive remanent ferroelectric state), and negative applied field, respectively. Clear voltage-induced domain structure changes are observed in each state. Edge identification was used in regions where we could unambiguously identify domains with the results for one grain shown in Figure 3g−j. We find that the domain wall density increases under the application of field compared to a zero field, poled film state, as shown in Figure 3k. For Grain 3, which is highlighted in Figure 3g−j, we observe increases of 9.9 and 10.2% in domain wall line length relative to the negatively poled state under fields of −414 and 414 kV/cm, respectively. The amount of domain boundary length change varied in the other grains measured, but we routinely observe greater than a 2% increase in domain wall length while the sample is under field. It is important to note that the 12 μm diameter of the laser spot used for the TDTR measurements results in a measurement volume that encompasses several adjacent grains, ensuring that the average increase in domain wall length/unit area is captured in each thermal measurement.

Combined, the PFM and SEM domain imaging data show that the domain wall densities increase after and during the application of a dc field. Increases in domain wall density in polycrystalline PZT thin films[30] and PZT bilayers,[24,29,31] similar to those studied here, have been observed previously between unpoled and poled states via PFM. Here, we show that domain wall density increases while under an applied field. This increase is a consequence of several factors, including interplay of ferroelectric switching and ferroelastic domains[30] and strain relief from the imposed mechanical boundary conditions that exist at grain boundaries and clamping to a rigid silicon substrate.[32] These increases in domain wall density correlate with decreases in thermal conductivity after poling into the remanent ferroelectric states and while under an electric field. The decreased thermal conductivity with increasing domain wall density results from increased phonon scattering across these interfaces. In addition to the increase in domain boundary area resulting in increased phonon scattering interfaces, an accompanying necessary decrease in domain wall spacing is likely to result in phonons of shorter mean free path lengths being scattered by domain walls, which may amplify this thermal conductivity tuning effect. Furthermore, as a consequence of the phonon scattering at domain boundaries mechanism, it can be anticipated that this tuning effect can occur at the time scale of ferroelastic switching, which has been shown to occur in the nanosecond time frame.[31,33] This indicates that the response time can be significantly faster than we have been able to measure using our experimental setup.

Finally, given the rich physics present in ferroelectrics, it is important to differentiate the effects observed in this work from electrocaloric effects. The application of a large electric field to a ferroelectric thin film results in a change in entropy and a concomitant change in temperature under adiabatic conditions.[34] The electrocaloric effect is a transient response that would not be observable over the several minute time scales of

DOI: 10.1021/nl504505t
Nano Lett. 2015, 15, 1791−1795

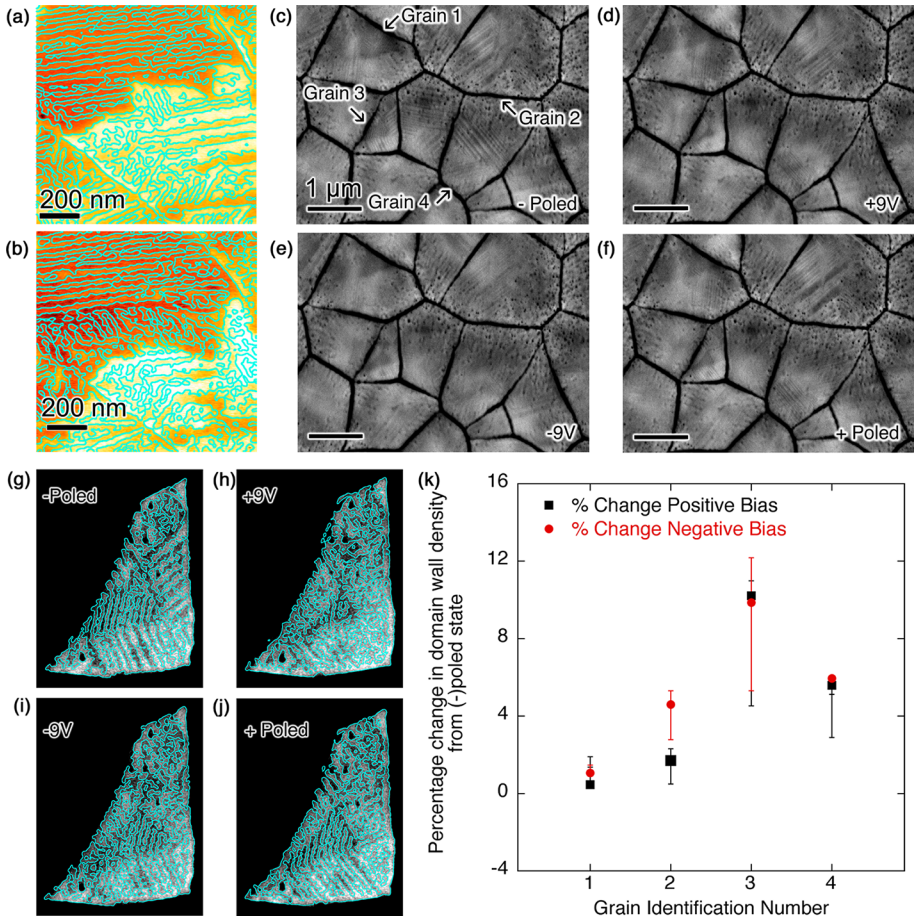

Figure 3. Piezoresponse force microscope images before (a) and after (b) application of an 8 V bias to the probe tip. The outlines on the images are the edge identification boundaries used to determine the percent change in domain wall area. An average domain wall density increase of 2.6% upon poling is observed. (c–f) Channeling contrast scanning electron micrographs of the bilayer PZT film in the negatively poled remanent state (c); with +9 V (~414 kV/cm) applied (d); with −9 V (~-414 kV/cm) applied (e); and in the positively poled remanent state (f). (g–j) The edge identification results for a specific grain from the channeling contrast SEM images in the same respective states as (c–f). (k) Measured relative change in domain wall density for the four grains highlighted in panel (d) while under positive bias (black squares) and negative bias (red circles).

our measurements, rather the response such as the locked-in thermal conductivity data in Figure 2b would decay with time and would have opposite sign temperature variations for applying and removing the electric field; that is, the temperature would increase quickly and then equilibrate while a field is applied and then decrease quickly and equilibrate upon removal of the field. That this was not observed suggests that electrocaloric effects constitute a minimal contribution to these measurements. The application of an electric field across a ferroelectric material may also decrease the heat capacity,[35] which would result in decreased thermal effusivity. This effect, however, is only significant at temperatures where there is a strong polarization dependence on temperature. The PZT compositions used in this study were measured at temperatures far from their phase transition temperatures (~400 and ~310 °C for $PbZr_{0.3}Ti_{0.7}O_3$ and $PbZr_{0.7}Ti_{0.3}O_3$, respectively) where this dependence is nearly zero. We measured the polarization response at multiple temperatures near room temperature, as shown in the Supporting Information, and no difference was observed, which precludes field-induced heat capacity changes from contributing to these results.

In summary, our results show that tens of nanometer-spaced ferroelastic domain boundaries in ferroelectric thin films may be used to alter phonon transport and prepare a voltage-actuated thermal switch or phonon transistor at temperatures well in excess of any previous demonstration. This effect can be used across broad temperature ranges and does not require altering the material composition or use of phase transitions. In addition, the dynamic tuning of thermal conductivity was found to be rapid and repeatable. We anticipate that through the application of domain structure engineering, nanosecond domain switching, and improved understanding of the phonon mean free path spectra in ferroelectric materials, this dynamic tuning effect could be further increased in amplitude and also potentially lead toward gigahertz tuning of phonons.

■ ASSOCIATED CONTENT

Supporting Information

Additional information on material synthesis, electrical and structural characterization, and TDTR measurements and data analysis. This material is available free of charge via the Internet at http://pubs.acs.org.

■ AUTHOR INFORMATION

Corresponding Authors

*E-mail: jihlefe@sandia.gov. Phone: 505-844-3162.
*E-mail: phopkins@virginia.edu. Phone: 434-982-6005.

DOI: 10.1021/nl504505t
Nano Lett. 2015, 15, 1791−1795

Author Contributions

J.I. and P.H. conceived the idea for this experiment and J.I. supervised all aspects of the experiment. B.F. and P.H. performed the thermal conductivity measurements and interpretation. J.I. and M.W. participated in the sample preparation. D.S., D.M., B.M., and J.M. performed microstructural characterization and measurement of domain structures. J.I., M.W., and S.T-M. analyzed film domain structure response to applied fields. The manuscript was written through contributions of all authors. All authors have given approval to the final version of the manuscript.

Notes

The authors declare no competing financial interest.

■ ACKNOWLEDGMENTS

This work was supported by the Laboratory Directed Research and Development (LDRD) program at Sandia National Laboratories, the Air Force Office of Scientific Research (FA9550-13-1-0067), and the National Science Foundation (CBET-1339436). Sandia National Laboratories is a multiprogram laboratory managed and operated by Sandia Corporation, a wholly owned subsidiary of Lockheed Martin Company, for the United States Department of Energy's National Nuclear Security Administration under contract DE-AC04−94AL85000. The authors wish to acknowledge the technical assistance of Mia Blea-Kirby, Garry Bryant, Benjamin Griffin, and John T. Gaskins. Critical review of this manuscript by Paul G. Clem, Thomas E. Beechem, and Jon-Paul Maria is greatly appreciated.

■ REFERENCES

(1) Li, N. B.; Ren, J.; Wang, L.; Zhang, G.; Hanggi, P.; Li, B. W. *Rev. Mod. Phys.* **2012**, *84* (3), 1045−1066.
(2) Dai, S.; Fei, Z.; Ma, Q.; Rodin, A. S.; Wagner, M.; McLeod, A. S.; Liu, M. K.; Gannett, W.; Regan, W.; Watanabe, K.; Taniguchi, T.; Thiemens, M.; Dominguez, G.; Neto, A. H. C.; Zettl, A.; Keilmann, F.; Jarillo-Herrero, P.; Fogler, M. M.; Basov, D. N. *Science* **2014**, *343* (6175), 1125−1129.
(3) Chang, C. W.; Okawa, D.; Majumdar, A.; Zettl, A. *Science* **2006**, *314* (5802), 1121−1124.
(4) Oh, D. W.; Ko, C.; Ramanathan, S.; Cahill, D. G. *Appl. Phys. Lett.* **2010**, *96* (15), 151906.
(5) Zheng, R. T.; Gao, J. W.; Wang, J. J.; Chen, G. *Nat. Commun.* **2011**, *2*, 289.
(6) Cho, J.; Losego, M. D.; Zhang, H. G.; Kim, H.; Zuo, J.; Petrov, I.; Cahill, D. G.; Braun, P. V. *Nat. Commun.* **2014**, *5*, 4035.
(7) Richardson, R. A.; Peacor, S. D.; Nori, F.; Uher, C. *Phys. Rev. Lett.* **1991**, *67* (27), 3856−3859.
(8) Steigmeir, E. F. *Phys. Rev.* **1968**, *168* (2), 523−530.
(9) Huber, W. H.; Hernandez, L. M.; Goldman, A. M. *Phys. Rev. B* **2000**, *62* (13), 8588−8591.
(10) Mante, A. J. H.; Volger, J. *Physica* **1971**, *52* (4), 577−604.
(11) Lin, F. Q.; Zhu, D. M. *Phys. Rev. B* **1994**, *49* (22), 16025−16027.
(12) Weilert, M. A.; Msall, M. E.; Anderson, A. C.; Wolfe, J. P. *Phys. Rev. Lett.* **1993**, *71* (5), 735−738.
(13) Daniels, J. E.; Jones, J. L.; Finlayson, T. R. *J. Phys. D: Appl. Phys.* **2006**, *39* (24), 5294−5299.
(14) Ni, Y.; Xiong, S.; Volz, S.; Dumitrică, T. *Phys. Rev. Lett.* **2014**, *113* (12), 124301.
(15) Holland, M. G. *Phys. Rev.* **1963**, *132* (6), 2461−2471.
(16) Henry, A. S.; Chen, G. *J. Comput. Theor. Nanosci.* **2008**, *5* (2), 141−152.
(17) Wang, Z. J.; Alaniz, J. E.; Jang, W. Y.; Garay, J. E.; Dames, C. *Nano Lett.* **2011**, *11* (6), 2206−2213.
(18) Cheaito, R.; Duda, J. C.; Beechem, T. E.; Hattar, K.; Ihlefeld, J. F.; Medlin, D. L.; Rodriguez, M. A.; Campion, M. J.; Piekos, E. S.; Hopkins, P. E. *Phys. Rev. Lett.* **2012**, *109* (19), 195901.
(19) Tachibana, M.; Kolodiazhnyi, T.; Takayama-Muromachi, E. *Appl. Phys. Lett.* **2008**, *93* (9), 092902.
(20) Foley, B. M.; Brown-Shaklee, H. J.; Duda, J. C.; Cheaito, R.; Gibbons, B. J.; Medlin, D.; Ihlefeld, J. F.; Hopkins, P. E. *Appl. Phys. Lett.* **2012**, *101* (23), 231908.
(21) Bisson, J. F.; Yagi, H.; Yanagitani, T.; Kaminskii, A.; Barabanenkov, Y. N.; Ueda, K. I. *Opt. Rev.* **2007**, *14* (1), 1−13.
(22) Donovan, B. F.; Foley, B. M.; Ihlefeld, J. F.; Maria, J.-P.; Hopkins, P. E. *Appl. Phys. Lett.* **2014**, *105* (8), 082907.
(23) Hopkins, P. E.; Adamo, C.; Ye, L. H.; Huey, B. D.; Lee, S. R.; Schlom, D. G.; Ihlefeld, J. F. *Appl. Phys. Lett.* **2013**, *102* (12), 121903.
(24) Anbusathaiah, V.; Kan, D.; Kartawidjaja, F. C.; Mahjoub, R.; Arredondo, M. A.; Wicks, S.; Takeuchi, I.; Wang, J.; Nagarajan, V. *Adv. Mater.* **2009**, *21* (34), 3497−3502.
(25) Cahill, D. G. *Rev. Sci. Instrum.* **2004**, *75* (12), 5119−5122.
(26) Schmidt, A. J.; Chen, X. Y.; Chen, G. *Rev. Sci. Instrum.* **2008**, *79* (11), 114902.
(27) Hopkins, P. E.; Serrano, J. R.; Phinney, L.; Kearney, S. P.; Grasser, T. W.; Harris, C. T. *J. Heat Transfer* **2010**, *132* (8), 081302.
(28) Stemmer, S.; Streiffer, S. K.; Ernst, F.; Ruhle, M. *Philos. Mag. A* **1995**, *71* (3), 713−724.
(29) Anbusathaiah, V.; Jesse, S.; Arredondo, M. A.; Kartawidjaja, F. C.; Ovchinnikov, O. S.; Wang, J.; Kalinin, S. V.; Nagarajan, V. *Acta Mater.* **2010**, *58* (16), 5316−5325.
(30) Ivry, Y.; Wang, N.; Chu, D. P.; Durkan, C. *Phys. Rev. B* **2010**, *81* (17), 174118.
(31) Ehara, Y.; Yasui, S.; Nagata, J.; Kan, D.; Anbusathaiah, V.; Yamada, T.; Sakata, O.; Funakubo, H.; Nagarajan, V. *Appl. Phys. Lett.* **2011**, *99* (18), 182906.
(32) Ivry, Y.; Chu, D. P.; Durkan, C. *Nanotechnology* **2010**, *21* (6), 065702.
(33) Li, J.; Nagaraj, B.; Liang, H.; Cao, W.; Lee, C. H.; Ramesh, R. *Appl. Phys. Lett.* **2004**, *84* (7), 1174−1176.
(34) Mischenko, A. S.; Zhang, Q.; Scott, J. F.; Whatmore, R. W.; Mathur, N. D. *Science* **2006**, *311* (5765), 1270−1.
(35) Benepe, J. W.; Reese, W. *Phys. Rev. B* **1971**, *3* (9), 3032−3039.

DOI: 10.1021/nl504505t
Nano Lett. 2015, 15, 1791−1795